Microsystem Technologies (2019) 25:3765–3777
https://doi.org/10.1007/s00542-019-04294-6

TECHNICAL PAPER

Enhanced backstepping sliding mode controller for motion tracking of a nonlinear 2-DOF piezo-actuated micromanipulation system

Amelia Ahmad Khalili[1] · Zaharuddin Mohamed[1] · Mohd Ariffanan Mohd Basri[1]

Received: 4 November 2018 / Accepted: 3 January 2019 / Published online: 13 January 2019

Abstract
In this paper a robust backstepping sliding mode controller is developed for tracking control of 2-DOF piezo-actuated micromanipulation system. The control approach is established to obtain high precision tracking in the existence of hysteresis nonlinearity, model uncertainties and external disturbances which treated as a lumped uncertainty. The control scheme is developed based on backstepping technique and a sliding surface is introduced in the final stage of the algorithm. To attenuate the chattering problem caused by a discontinuous switching function, a simple fuzzy system is used. The asymptotical stability of the system can be guaranteed since the control law is derived based on Lyapunov theorem. The effectiveness and feasibility of the suggested approach are tested for tracking of a micrometer-level reference trajectories. From the results, it is shown that the developed control system not only achieves satisfactory control performance, but also eliminates the chattering phenomena in the control effort.

1 Introduction

Micromanipulation systems with piezoelectric actuation are widely employed in diverse applications. In biological or biomedical applications for instance, the piezo-driven micromanipulation systems are employed to handle microscopic specimens and also being used in cell microinjection operation. Piezoelectric actuator has major advantages such as micrometer scale resolution, high stiffness and rapid response speed. Hence, piezoelectric actuators have been extensively adopted in the aforementioned applications. Nevertheless, the major challenge of using piezo-actuated micromanipulation systems arises from the piezoelectric hysteresis nonlinearity effect. The hysteresis can induce considerable large error and deteriorate the performance of such systems in terms of accuracy and speed. Hence, the hysteresis should be suppressed to achieve a precision control.

Various control strategies involving feedforward and feedback technique have been proposed to compensate for the undesirable hysteresis effect of the PEA. On the other hand, a number of hysteresis models such as the Preisach model (Stakvik et al. 2015; Yu et al. 2002), the Maxwell resistive capacitor model (Lee et al. 2000; Liu et al. 2013), the Duhem model (Zhou and Wang 2013; Xie et al. 2009), the Bouc–Wen model (Ikhouane and Rodellar 2005; Rakotondrabe 2011), and the Prandtl–Ishlinskii model (Elahinia et al. 2012; Liu 2012) have been developed in order to facilitate the design of controllers. In the feedforward control, hysteresis is compensated using an inverse of the hysteresis models. However, a precise hysteresis model is necessary for feedforward control techniques in order to effectively alleviate the effect of hysteresis.

By considering that modeling the hysteresis is a complicated work and it is difficult to obtain precise hysteresis model, feedback control techniques have been adopted. In this approach, the hysteresis nonlinearity can be described as additional uncertainty terms added to the nominal model of the system and the control algorithm is then devised to suppress the uncertainties. Numerous feedback-based control techniques like linear quadratic regulator (LQR) control (Thomas and Gopinath 2016; de Oliveira et al. 2015), proportional–integral–derivative (PID) control (Ding et al. 2016; Youssef 2013; Lin et al. 2011), H-infiniti control (Ahmad and Abdurraqeeb 2017; Lee et al. 2010; Xiao and Li 2014), sliding mode control (SMC) (Shen et al. 2008; Yang et al. 2014; Xu 2014), feedback linearization control (Adriaens and Banning 1999; Onawola and Sinha

✉ Mohd Ariffanan Mohd Basri
ariffanan@fke.utm.my

[1] School of Electrical Engineering, Faculty of Engineering, Universiti Teknologi Malaysia, UTM Johor Baharu, 81310 Johor Baharu, Malaysia

2011), fuzzy logic control (Badr and Ali 2010; Li et al. 2012; Shabaninia and Mavaddat 2014), neural network control (Svečko and Kusić 2015; Čas et al. 2010) and backstepping control (Payam et al. 2009) have been developed for compensating the hysteresis nonlinearity effects in PEA.

The backstepping control scheme is a nonlinear control method based on the Lyapunov theorem. The backstepping control design techniques have received great attention because of its systematic and recursive design methodology for nonlinear feedback control. The backstepping control approach also has been successfully implemented in numerous real-world applications such as ship (Witkowska and Smierzchalski 2007), vehicle suspension system (Ranaweera et al. 2013), offshore platform (Liang and Liu 2012), power system (Chan and Nguang 2002), electronic throttle system (Bai et al. 2013), electrohydraulic actuator (Toader and Ursu 2007) and two-wheeled mobile manipulator (Acar and Murakami 2008). Unlike the feedback linearization method with the problems such as the precise model requirement and the cancellation of useful nonlinear terms, the backstepping approach offers a choice of design tools for accommodation of nonlinearities, and can avoid unwanted cancellations. The advantage of backstepping compared with other control methods lies in its design flexibility, due to its recursive use of Lyapunov functions. The key idea of the backstepping design is to select recursively some appropriate state variables as virtual inputs for lower dimension subsystems of the overall system and the Lyapunov functions are designed for each stable virtual controller (Krstic et al. 1995). Therefore, the designed final actual control law can guarantee the stability of the total control system.

Although the nonlinear control realized by backstepping method can meet the desired performance of the system, but it is just limited to the nominal system i.e., the system dynamic model and the external disturbance are exactly known. Hence, the motivation of this work is to design a new backstepping-based robust control approach for a 2-DOF piezo-actuated micromanipulation system with uncertainties. Robust control methods have been extensively investigated to handle unknown uncertainties that arise in a system. SMC for example, has proven to be very robust to model uncertainties and external disturbances. Thus, owing to the merits of backstepping control and SMC, in this paper, both control schemes are combined for tracking control of a 2-DOF piezo-actuated micromanipulation system. In the design, an SMC scheme is introduced in the final step of backstepping method. Nevertheless, a discontinuous sign function of sliding manifold will excite undesired phenomena called chatter in the control input. The chatter can deteriorate system performance and also cause undesired wear and tear in micromechanical devices. Therefore, it is essential to develop a strategy to eliminate the chatter in the control input. To solve the issue, a simple fuzzy system which proposed in (Wai 2007) is utilized to replace the sign function. By doing this, the chatter is eliminated effectively, because the control input is smooth with respect to time. To demonstrate the effectiveness and feasibility of the developed control strategy, a simulation of 2-DOF piezo-actuated micromanipulation system with uncertainties is examined. Compared with the method presented in Payam et al. (2009) and Shen et al. (2008), the developed control scheme has respectively the advantage of robustness and free from the chattering phenomena, which makes this approach attractive for a wide class of nonlinear systems with the influences of uncertainties. The main contribution of this paper is a successful development of a robust chattering free backstepping sliding mode controller for a 2-DOF piezo-actuated micromanipulation system with uncertainties. The originality of this work relies on the technique to compensate the uncertainties present on the piezo-actuated micromanipulation system. In this approach, a simple fuzzy system is introduced to mimic the hitting control effort that used to compensate the effect of uncertainties. Additionally, the stability analysis for the designed controller is theoretically proven by the Lyapunov theory. Therefore, the proposed controller can guarantee the stability of the closed-loop system and improve the robustness against uncertainties.

2 Model of 2-DOF piezo-actuated micromanipulation system

The aim of this paper being the control of a 2-DOF piezo-actuated micromanipulation system devoted to precise positioning. To achieve biaxial precision tracking tasks, two piezo-actuated translation stages are adapted to be a 2-DOF piezo-actuated micromanipulation system. Each piezo-actuated translation stage is comprised of the moving stage (MS) and the piezoelectric actuator (PEA) as shown in Fig. 1. The MS is modeled as a second-order linear dynamics referring to the mass-spring-damper system, and the PEA can be regarded as a nonlinear part of the dynamics, representing the hysteresis nonlinearity effect. The model merges mass-spring-damper with a nonlinear hysteresis function which appears in the input excitation to the system. The modeling of the MS can be formulated as the follows:

$$m\ddot{x} + b\dot{x} + kx = F_{PZT}, \tag{1}$$

where the symbols denotes: x as the displacement of the stage. $\dot{x}$, $\ddot{x}$, respectively, as the first and second order derivatives of x with respect to time, t. m as the mass of MS. b as the stiffness of MS. k as the damper coefficient of MS. F_{PZT} as the force generated by the PEA.

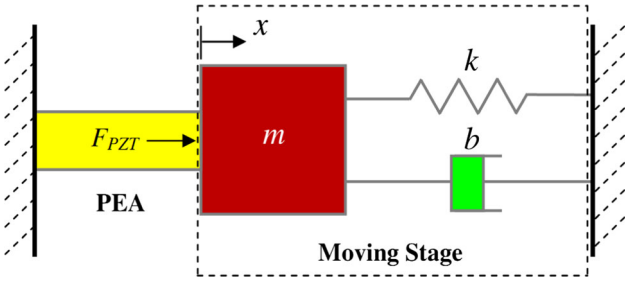

Fig. 1 Model of the piezo-actuated translation stage

Nevertheless, the correlation between the actuated force F_{PZT} and the applied voltage V is nonlinear due to the hysteresis phenomena of PEA. Thus, the dynamic of hysteresis should be formulated using the nonlinear differential equations to overcome the drawback.

In order to describe the nonlinearity of the PEA, Bouc–Wen model is chosen in this work. It is due to the model's simplicity involving fewer parameters which make it easier for the integration with the rest of the model. Furthermore, the Bouc–Wen model has also been verified to be suitable to represent the PEA's hysteresis loop (Low and Guo 1995; Li and Xu 2010). Consequently, the PEA modeling could be formulated as follows (Lin and Yang 2006):

$$\begin{cases} F_{PZT} = k(dV - h) \\ \dot{h} = \alpha d\dot{V} - \beta|\dot{V}|h - \gamma\dot{V}|h| \end{cases}, \tag{2}$$

where the symbols signifies, h as the hysteretic nonlinear term. $\dot{h}$ as the derivatives of h with respect to time t. V as the applied voltage. d as the ratio of the displacement to the applied voltage. α, β, γ as the parameters to determine the hysteretic loops' magnitude and shape.

The modeling of the piezo-actuated translation stage dynamics could be described by the following second-order nonlinear system by substituting (1) into (2):

$$\begin{cases} m\ddot{x} + b\dot{x} + kx = k(dV - h) \\ \dot{h} = \alpha d\dot{V} - \beta|\dot{V}|h - \gamma\dot{V}|h| \end{cases}. \tag{3}$$

Figure 2 shows the block diagram representing (3).

Model (3) is valuable for 1-DOF piezo-actuated micromanipulation system of the x-axis motion. The axes of displacement of the 2-DOF piezo-actuated micromanipulation system are x and y. If there are no cross-couplings between the two axes, the each axis can be treated independently. Thus, two single-input and single-output controllers can be employed for the x- and y-axis of the piezo-actuated micromanipulation system, respectively. For the sake of brevity, only the treatment of x-axis motion is presented in this paper.

By rearranging (3), the following dynamic can be obtained:

$$\ddot{x} = -\frac{b}{m}\dot{x} - \frac{k}{m}x + \frac{kd}{m}V - \frac{kh}{m}. \tag{4}$$

From (4), the integrated hysteresis apparently shows that the dynamics of the piezo-actuated translation stage is a nonlinear system. Therefore, a voltage-to-displacement curve simulation result is provided in Fig. 3, with the aim to validate the feasibility of the investigated hysteresis model shown in (4). The system parameters values are implemented from (Huang and Lin 2004) as given in Table 1, and the sinusoidal input voltage is applied to the hysteresis model with amplitude 50 V and frequency 0.25 Hz.

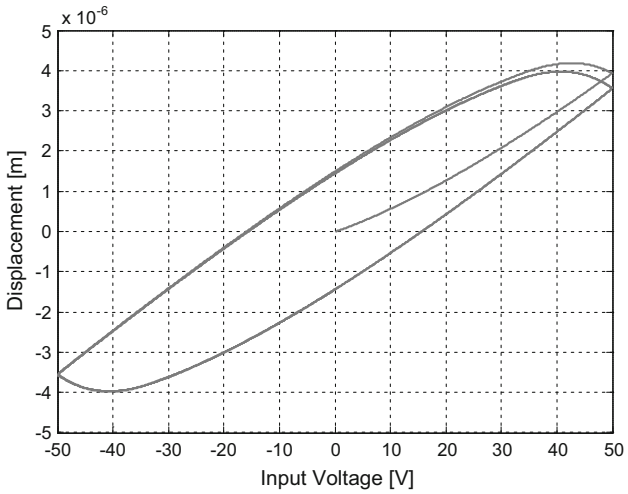

Fig. 3 Hysteresis loops simulation

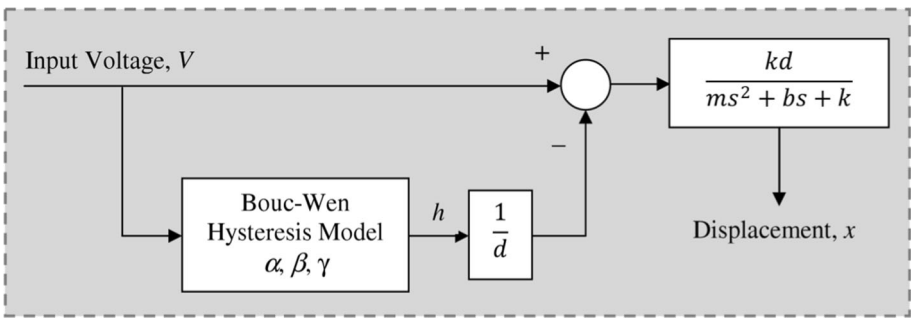

Fig. 2 The piezo-actuated translation stage with hysteresis block diagram

Table 1 Parameters value of the piezo-actuated translation stage

Physical parameters	Symbol	Value	Units
Mass	m	5	kg
Viscous damping coefficient	b	20.144×10^{3}	N s/m
Stiffness factor	k	5×10^{6}	N/m
Ratio of the displacement to voltage	d	1.1452×10^{-7}	m/V
Hysteresis parameter	α	0.365	
Hysteresis parameter	β	0.0485	
Hysteresis parameter	γ	− 0.0221	

Figure 3 discloses that the hysteresis effect of the PEA could be modeled by the suggested hysteresis model which is incorporated within the overall dynamics of the piezo-actuated translation stage.

The dynamic Eq. (4) can be written in the following affine state representation such as:

$$\ddot{x} = f(x) + g(x)u, \tag{5}$$

where the input, nonlinear dynamic function and control function, respectively are u, $f(x)$ and $g(x)$ specified as:

$$u = V, \tag{6}$$

$$f(x) = -\frac{b}{m}\dot{x} - \frac{k}{m}x - \frac{kh}{m}, \tag{7}$$

$$g(x) = \frac{kd}{m}. \tag{8}$$

The nominal model of nonlinear system (5) could be presented as follows, with the assumption that all the parameters of the system are well known:

$$\ddot{x} = f_o(x) + g_o(x)u, \tag{9}$$

where the nominal value of f and g, respectively are f_o and g_o.

If system uncertainties are exist, there will be deviation in the system's parameters from the nominal value and the addition of external disturbance into the system. Therefore, the nonlinear system (5) could be expressed as:

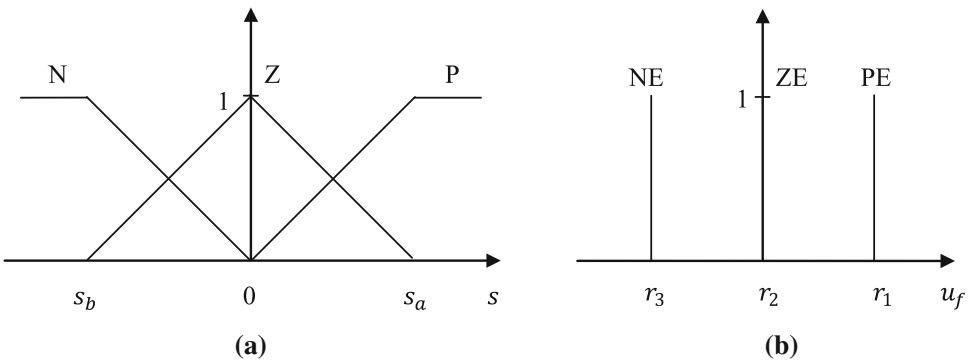

Fig. 4 Membership functions. **a** Input fuzzy sets. **b** Output fuzzy sets

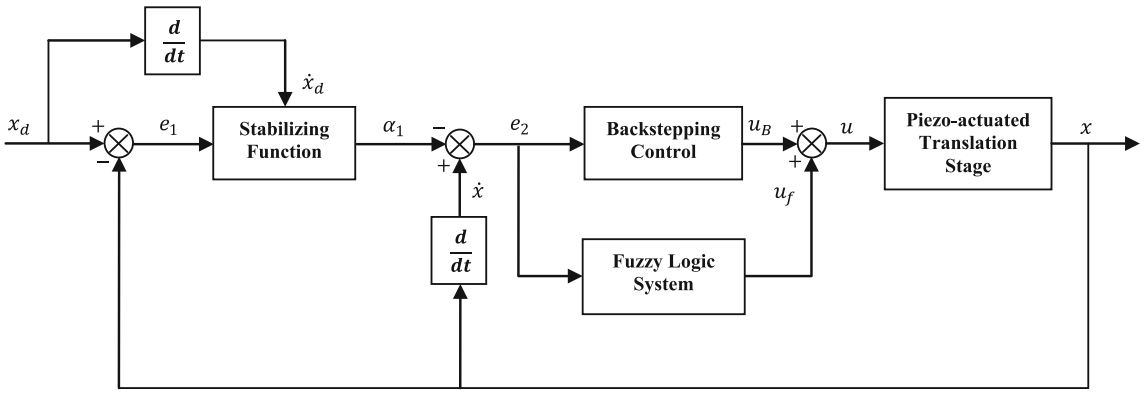

Fig. 5 Block diagram of the chattering free backstepping sliding mode control system

$$\begin{aligned}\ddot{x} &= [f_o(x) + \Delta f(x)] + [g_o(x) + \Delta g(x)]u + \delta \\ &= f_o(x) + g_o(x)u + L\end{aligned}, \tag{10}$$

where the unknown uncertainties are signifies by $\Delta f(x)$ and $\Delta g(x)$, and the unknown external disturbance represented by δ. Lumped uncertainty denotes by L which comprises the nonlinear additive uncertainties and an external disturbance, which are defined as $L = \Delta f(x) + \Delta g(x)u + \delta$. The bound of lumped uncertainty L is assumed to be given, that is $|L| \leq \beta$, where β is a given positive constant.

3 Backstepping sliding mode control design

The aim is to construct a suitable control law for system (3) so that even in the presence of unknown uncertainties the piezo-actuated translation stage can still track any desired reference trajectory, denoted by x_d.

3.1 Ideal backstepping control (IBC)

The strategy of backstepping control (BC) for the piezo-actuated translation stage is explained step-by-step in the following:

Step 1 Tracking error definition:

$$e_1 = x_d - x, \tag{11}$$

where x_d represented the desired trajectory specified by a reference model. The tracking error derivative is presented as:

$$\dot{e}_1 = \dot{x}_d - \dot{x}. \tag{12}$$

The selections of the first Lyapunov function as:

$$V_1(e_1) = \frac{1}{2}e_1^2. \tag{13}$$

The derivative of V_1 is:

$$\dot{V}_1(e_1) = e_1\dot{e}_1 = e_1(\dot{x}_d - \dot{x}) \tag{14}$$

$\dot{x}$ could be viewed as a virtual control. A stabilizing function recognized by the desired value of virtual control is described as:

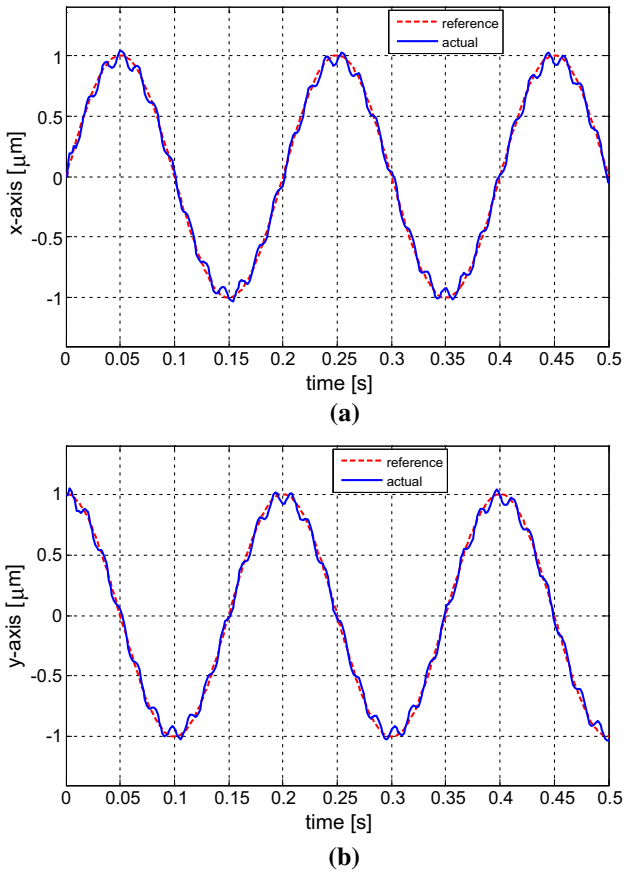

Fig. 6 Position tracking with frequency of 5 Hz using BC in **a** x-axis and **b** y-axis

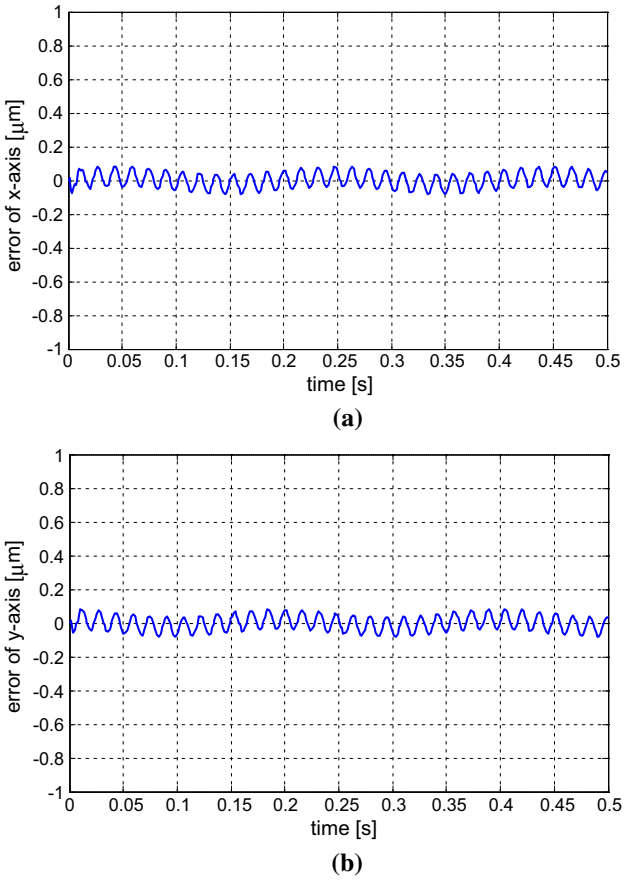

Fig. 7 Tracking errors with frequency of 5 Hz using BC in **a** x-axis and **b** y-axis

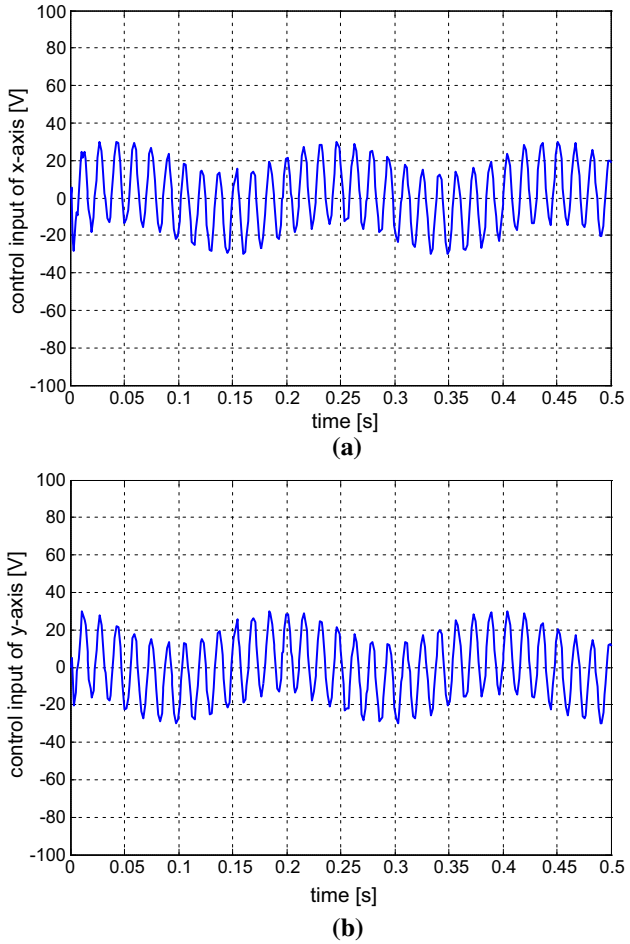

Fig. 8 Control inputs with frequency of 5 Hz using BC in **a** x-axis and **b** y-axis

$$\alpha = \dot{x}_d + k_1 e_1, \tag{15}$$

where k_1 is a positive constant.

By substituting the virtual control by its desired value, Eq. (14) is arranged to be:

$$\dot{V}_1(e_1) = -k_1 e_1^2 \leq 0. \tag{16}$$

Step 2 The deviation of the virtual control from its desired value can be described as:

$$e_2 = \dot{x} - \alpha = \dot{x} - \dot{x}_d - k_1 e_1. \tag{17}$$

The derivative of e_2 is represented as:

$$\begin{aligned} \dot{e}_2 &= \ddot{x} - \dot{\alpha} \\ &= f_o(x) + g_o(x)u + L - \ddot{x}_d - k_1 \dot{e}_1 \end{aligned}. \tag{18}$$

The second Lyapunov function is selected as:

$$V_2(e_1, e_2) = \frac{1}{2} e_1^2 + \frac{1}{2} e_2^2. \tag{19}$$

Determining derivative for (19), produces:

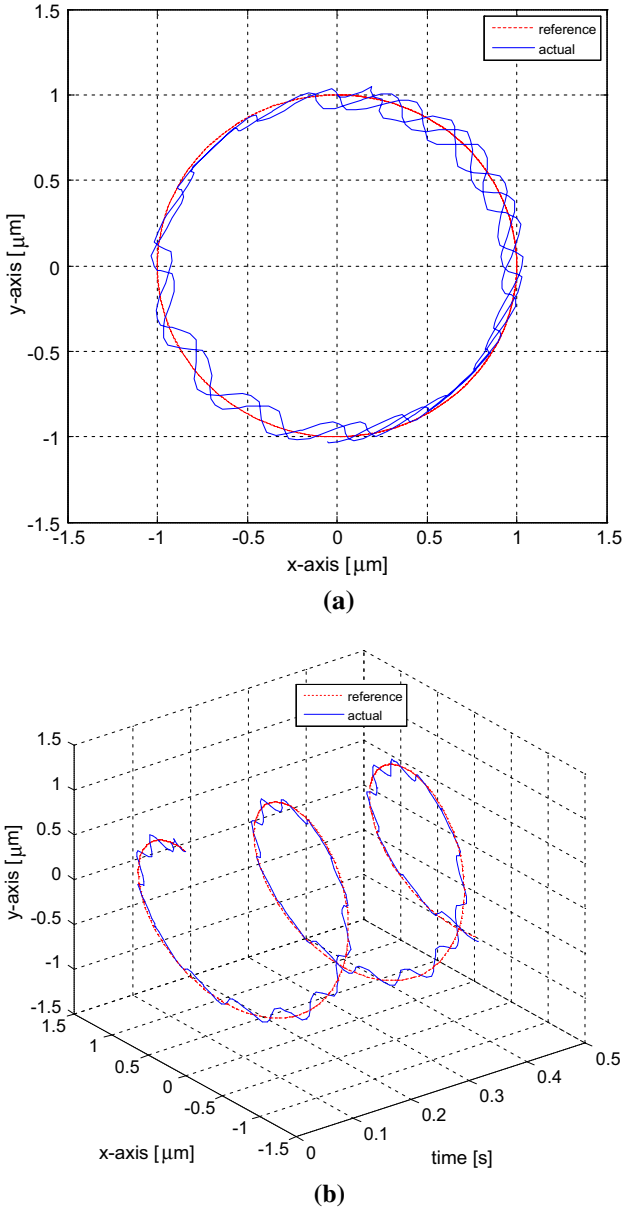

Fig. 9 Circular trajectory tracking response with frequency of 5 Hz using BC in **a** 2D and **b** 3D

$$\begin{aligned} \dot{V}_2(e_1, e_2) &= e_1 \dot{e}_1 + e_2 \dot{e}_2 \\ &= e_1(\dot{x}_d - \dot{x}) + e_2(\ddot{x} - \dot{\alpha}) \\ &= e_1(-e_2 - k_1 e_1) + e_2(f_o(x) + g_o(x)u + L - \ddot{x}_d - k_1 \dot{e}_1) \\ &= -k_1 e_1^2 + e_2(-e_1 + f_o(x) + g_o(x)u + L - \ddot{x}_d - k_1 \dot{e}_1). \end{aligned} \tag{20}$$

Step 3 By considering the system dynamics and the external disturbance are well identified, the ideal BC law could be acquired as:

$$u_{ibc} = \frac{1}{g_o(x)}(e_1 + k_1 \dot{e}_1 + \ddot{x}_d - f_o(x) - L - k_2 e_2), \tag{21}$$

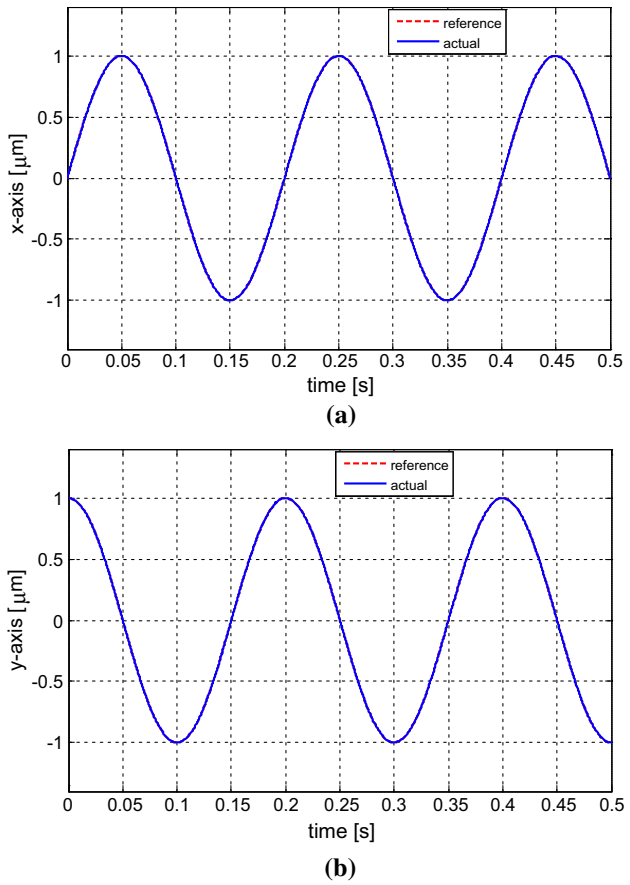

Fig. 10 Position tracking with frequency of 5 Hz using EBSMC in **a** x-axis and **b** y-axis

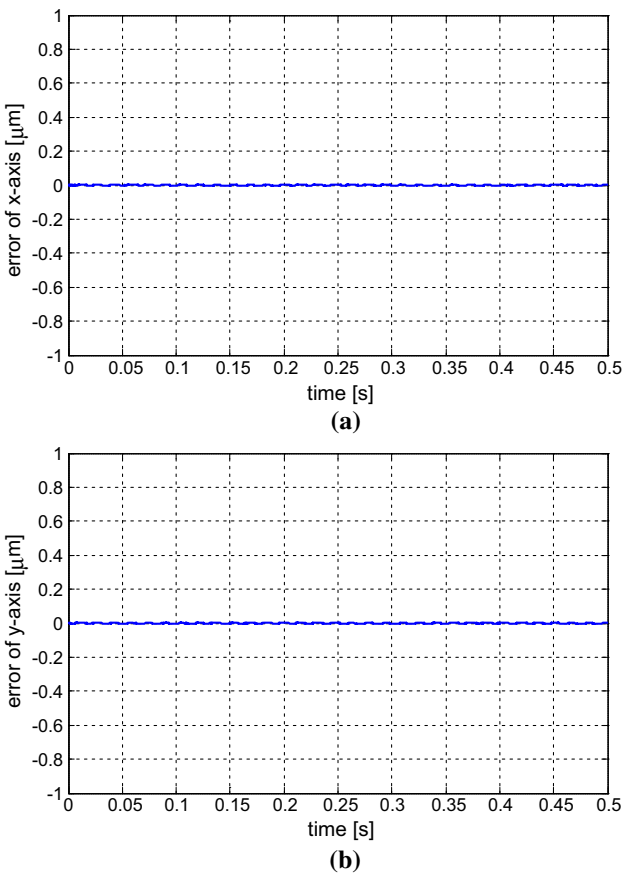

Fig. 11 Tracking errors with frequency of 5 Hz using EBSMC in **a** x-axis and **b** y-axis

where the positive constant is represented by k_2 is a. The stabilization of tracking error e_1 is performed by adding the term $k_2 e_2$.

The following equation could be achieved by substituting (21) into (20):

$$\dot{V}_2(e_1, e_2) = -k_1 e_1^2 - k_2 e_2^2 = -E^T K E \leq 0, \tag{22}$$

where $E = [e_1 e_2]^T$ and $K = diag(k_1, k_2)$. Since $\dot{V}_2(e_1, e_2) \leq 0$, $\dot{V}_2(e_1, e_2)$ is negative semi-definite, the following term is arranged as:

$$\Omega(t) = E^T K E = -\dot{V}_2(e_1, e_2). \tag{23}$$

By integrating $\Omega(t)$ with respect to time, the following is acquired:

$$\int_0^t \Omega(\tau) d\tau \leq V_2(e_1, e_2, 0) - V_2(e_1, e_2, t). \tag{24}$$

Since $V_2(e_1, e_2, 0)$ is bounded, and $V_2(e_1, e_2, t)$ is non-increasing and bounded, resulting follows:

$$\lim_{t \to \infty} \int_0^t \Omega(\tau) d\tau < \infty. \tag{25}$$

Furthermore, $\dot{\Omega}(\tau)$ is also bounded, therefore by using Barbalat's lemma (Astrom and Wittenmark 1995), the subsequent outcome could be achieved:

$$\lim_{t \to \infty} \Omega(\tau) = 0. \tag{26}$$

That is e_1 and e_2 will converge to zero as $t \to \infty$.

Therefore, the system able to be stabilized asymptotically using the control law in (21).

3.2 Backstepping sliding mode control (BSMC)

In practical application, since the lumped uncertainty L is commonly unknown, hence, the BC law (21) cannot ensure the favorable control performance. Thus, auxiliary control effort should be designed to eliminate the effect of the lumped uncertainty. The auxiliary control effort is referred as hitting control effort represented by u_H. The hitting control effort is designed such that the system state

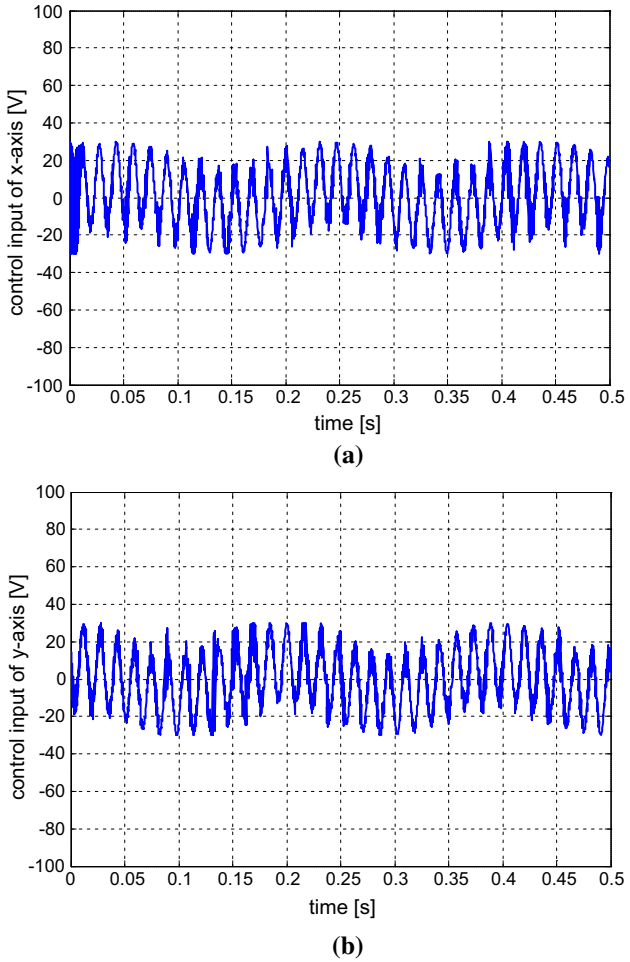

Fig. 12 Control inputs with frequency of 5 Hz using EBSMC in **a** *x*-axis and **b** *y*-axis

trajectories are forced toward the sliding surface and stay on it. This effort is known as the sliding mode.

Procedures to design of the backstepping sliding mode control (BSMC) can be described by the following steps:

Step 1 Similar as Step 1 in the design of ideal backstepping control (IBC).

Step 2 Define a sliding surface in terms of the error such as:

$$s = e_2 = \dot{x} - \dot{x}_d - k_1 e_1. \tag{27}$$

Thus, the Lyapunov function (19) can be written as:

$$V_2 = \frac{1}{2} e_1^T e_1 + \frac{1}{2} s^T s. \tag{28}$$

Differentiating (28) with respect to time leads to:

$$\begin{aligned} \dot{V}_2 &= e_1^T \dot{e}_1 + s^T \dot{s} \\ &= e_1^T(-e_2 - k_1 e_1) + s^T(f(x) + g(x)u + L - \ddot{x}_d - k_1 \dot{e}_1) \\ &= -k_1 e_1^T e_1 + s^T(-e_1 + f(x) + g(X)u + L - \ddot{x}_d - k_1 \dot{e}_1). \end{aligned} \tag{29}$$

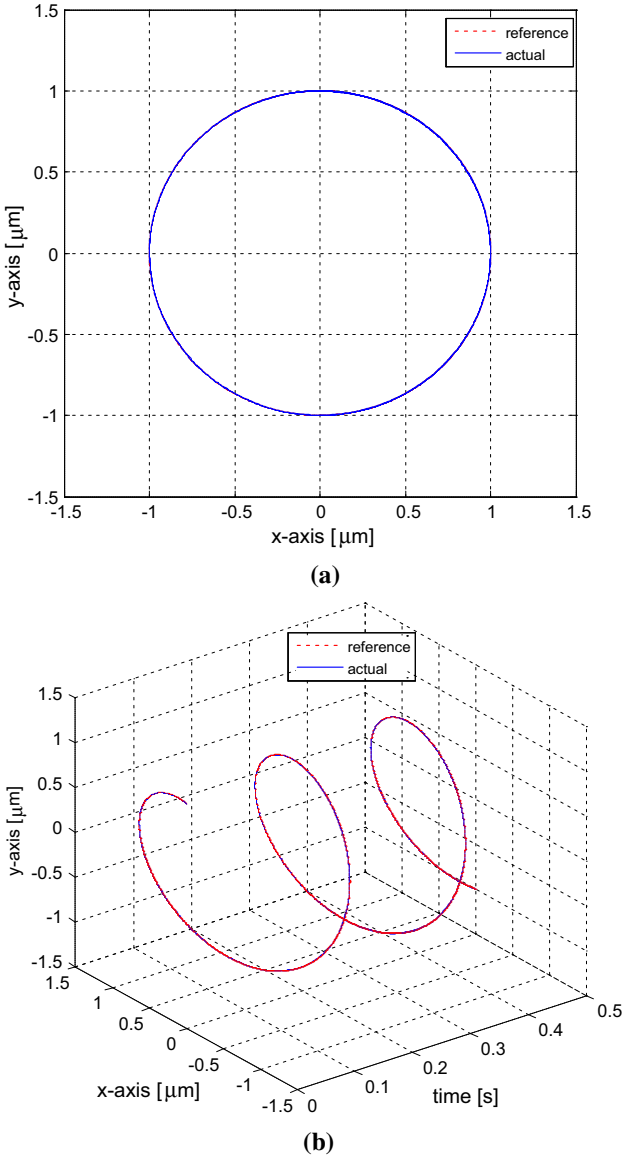

Fig. 13 Circular trajectory tracking response with frequency of 5 Hz using EBSMC in **a** 2D and **b** 3D

Step 3 Since the lumped uncertainty is unknown, a backstepping control can be obtained as:

$$u_B = \frac{1}{g(x)}(e_1 + k_1 \dot{e}_1 + \ddot{x}_d - f(x) - k_2 s). \tag{30}$$

Step 4 Define the hitting control effort such as:

$$u_H = \lambda sign(s), \tag{31}$$

where λ is a constant and $sign(s)$ is a sign function:

$$sign(s) = \begin{cases} 1, s/\rho > 0 \\ -1, s/\rho < 0 \end{cases}. \tag{32}$$

Totally, the robust control law known as backstepping sliding mode control law for nonlinear systems with the

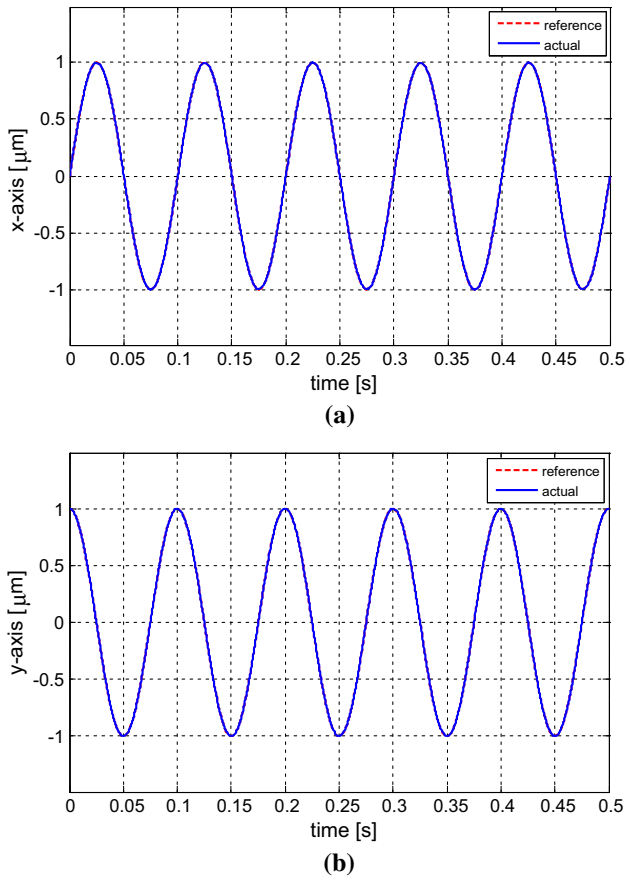

Fig. 14 Position tracking with frequency of 10 Hz using EBSMC in **a** x-axis and **b** y-axis

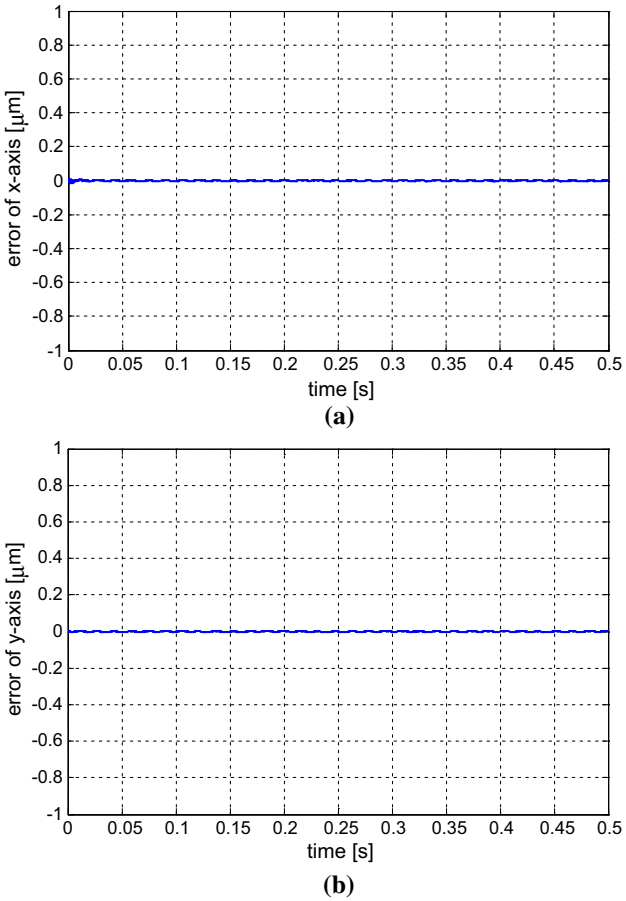

Fig. 15 Tracking errors with frequency of 10 Hz using EBSMC in **a** x-axis and **b** y-axis

present of lumped uncertainty, which guarantees the stability and convergence can be represented as:

$$u = u_B + u_H = \frac{1}{g(x)}(e_1 + k_1\dot{e}_1 + \ddot{x}_d - f(x) - k_2 s) + \lambda sign(s). \quad (33)$$

3.3 Enhanced backstepping sliding mode control (EBSMC)

The utilization of discontinuous sign function will excite undesired phenomenon called chatter. In order to eliminate the chattering phenomena, a simple fuzzy system is utilized to mimic the hitting control effort. Let the sliding surface s be the input linguistic variable of the fuzzy logic system, and the hitting control effort u_f be the output linguistic variable. To reduce the calculation, the hitting control effort is designed by three simple fuzzy rules as given in the following form (Wai 2007):

Rule 1 : IF s P THEN u_f is PE, (34)

Rule 2 : IF s Z THEN u_f is ZE, (35)

Rule 3 : IF s N THEN u_f is NE, (36)

where the triangular-typed functions and singletons are used to define the membership functions of IF-part and THEN-part, which are depicted in Fig. 4a and b, respectively.

The defuzzification of the output is accomplished by the method of center-of-gravity as follows:

$$u_f = \frac{\sum_{i=1}^{3} r_i w_i}{\sum_{i=1}^{3} w_i} = r_1 w_1 + r_2 w_2 + r_3 w_3, \quad (37)$$

where $0 \le w_1 \le 1$, $0 \le w_2 \le 1$ and $0 \le w_3 \le 1$ are the firing strengths of rules 1, 2 and 3, respectively; $r_1 = r$, $r_2 = 0$ and $r_3 = -r$ are the center of the membership functions PE, ZE and NE, respectively. The relation $w_1 + w_2 + w_3 = 1$ is valid according to the special case of triangular membership function-based fuzzy system. Hence, the following four conditions can be deduced. For any value of input s, only one of four conditions will occur according to Fig. 4a (Wai 2007).

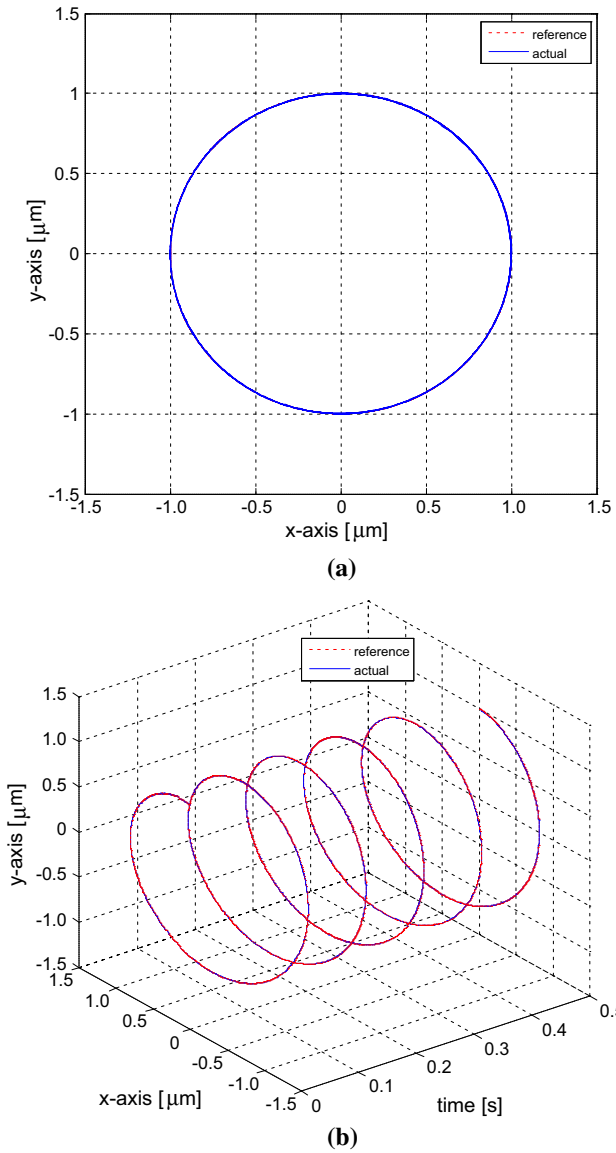

Fig. 16 Circular trajectory tracking response with frequency of 10 Hz using EBSMC in **a** 2D and **b** 3D

Condition 1 Only rule 1 is triggered. $(s > s_a, w_1 = 1, w_2 = w_3 = 0)$

$$u_f = r_1 = r. \tag{38}$$

Condition 2 Rules 1 and 2 are triggered simultaneously. $(0 < s \le s_a, 0 < w_1, w_2 \le 1, w_3 = 0)$

$$u_f = r_1 w_1 = r w_1. \tag{39}$$

Condition 3 Rules 2 and 3 are triggered simultaneously. $(s_b < s \le 0, w_1 = 0, 0 < w_2, w_3 \le 1)$

$$u_f = r_3 w_3 = -r w_3. \tag{40}$$

Condition 4 Only rule 3 is triggered. $(s \le s_b, w_1 = w_2 = 0, w_3 = 1)$

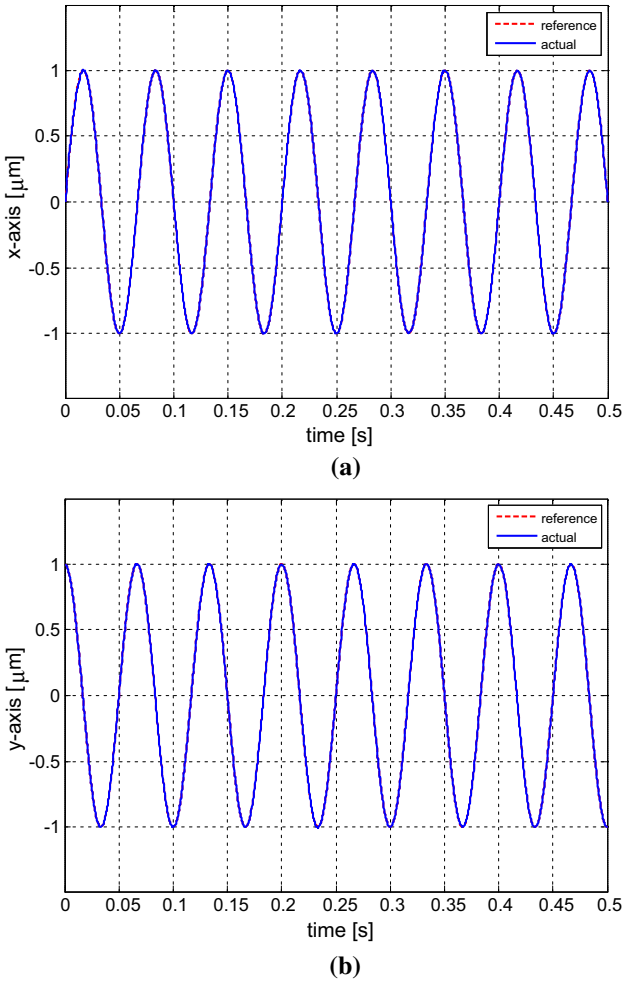

Fig. 17 Position tracking with frequency of 15 Hz using EBSMC in **a** x-axis and **b** y-axis

$$u_f = r_3 = -r. \tag{41}$$

According to four possible conditions, the (38)–(41) can be rewritten as:

$$u_f = r(w_1 - w_3). \tag{42}$$

Totally, the control law for a piezo-actuated translation stage with the present of lumped uncertainty can be represented as:

$$u = u_B + u_f = \frac{1}{g(x)}\left(e_1 + k_1\dot{e}_1 + \ddot{x}_d - f(x) - k_2 e_2\right) + r(w_1 - w_3). \tag{43}$$

Theorem *For the nonlinear dynamic equation of piezo-actuated translation stage with lumped uncertainty as represented by (10), if the control law in (43) is applied, the system will asymptotically stable.*

Proof Consider the Lyapunov function (28) and its derivative (29).

Substituting the control law from (43), then (29) becomes:

$$\begin{aligned}\dot{V}_2 &= -k_1 e_1^T e_1 - k_2 s^T s + sg(x)r(w_1 - w_3) + sL \\ &= -k_1 e_1^T e_1 - k_2 s^T s + |s|(r|g(x)||w_1 - w_3| + L)\end{aligned}. \quad (47)$$

Hence, the design parameter should be chosen in such a way that $\dot{V}_2 \leq 0$ is always satisfied. As aforementioned, it is assumed that L is bounded with β.

If the following inequality holds:

$$-r > \frac{\beta}{|g(x)||(w_1 - w_3)|}, \quad (48)$$

then $\dot{V}_2 \leq 0$ can be guaranteed.

The configuration of the developed control system is depicted in Fig. 5.

4 Results and discussion

This section discussed the performance of the proposed approach by conducting and evaluating the simulation study. Model parameter values of the piezo-actuated micromanipulation system are obtained from (Huang and Lin 2004) such as listed in Table 1. Two different simulation approach have been conducted on the piezo-actuated micromanipulation system with the influences of uncertainties. The first experiment provides the simulation results of the piezo-actuated micromanipulation system for the circular trajectory tracking control. The traditional backstepping control (Payam et al. 2009) is also selected to correlate with the results obtained by the developed EBSMC. The second experiment investigated the feasibility and effectiveness of the designed controller for tracking in a difference working frequencies.

4.1 Simulation 1: circular trajectory tracking

The circular motion trajectory with frequency of 5 Hz is used to evaluate the performance of the motion control system. The tracking performances of the circular motion trajectory with center (0, 0) μm and radius 1 μm by using traditional BC and by using the EBSMC are evaluated. The simulation results of the circular trajectory tracking for BC approach under the influences of uncertainties are shown in Figs. 6, 7, 8 and 9. Meanwhile, the simulation results of the circular trajectory tracking for EBSMC approach under the influences of uncertainties are shown in Figs. 10, 11, 12 and 13. As can be seen in Fig. 6, the traditional BC is unable to track the desired reference trajectory accurately.

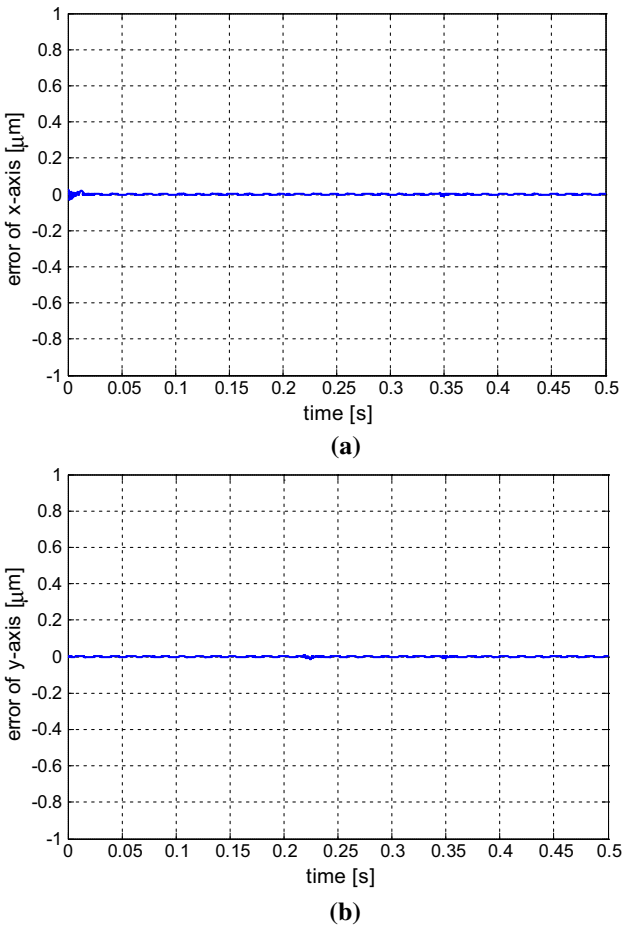

Fig. 18 Tracking errors with frequency of 15 Hz using EBSMC in **a** x-axis and **b** y-axis

The traditional BC give errors with the bound values of ±0.1 (μm) for both x- and y-axes as shown in Fig. 7. The control signal for the BC is depicted in Fig. 8 and the spatial curves are pictured in Fig. 9. Compared to BC, the proposed controller give a higher tracking performance as shown in Fig. 10. As can be seen in Fig. 11, the tracking error values produced by EBSMC mostly lied within ±0.01 (μm) for both x- and y-axes which lower than the value from BC technique. The improved performance of EBSMC over BC is due to its ability to compensate the uncertainties. The use of robust compensator has provided the capability of the proposed controller to deal with uncertainties. The control signals of the proposed controller is shown in Fig. 12. It can be shown that, the control chattering of the proposed controller is almost eliminated. By using a simple fuzzy system to replace the discontinuous sign function, it is shown that the control chatters can be attenuated. Figure 13 depicts the spatial curve which show the micromanipulation system well tracks the circular reference trajectory by using EBSMC.

4.2 Simulation 2: effect of different frequency

To analyze the capacity of the proposed controller to track higher frequencies for the circular trajectory, an experiments with 10 Hz and 15 Hz are also carried out. The results are depicted in Figs. 14, 15, 16, 17, 18 and 19. It shows that the tracking error remains almost similar than with low frequency. The tracking performance with reference to frequencies of 10 Hz and 15 Hz are seen in Figs. 14 and 17, respectively. As can be seen, the proposed controller still can provide a good performance with high tracking accuracy and robust performance as frequency become faster. The trajectory tracking error of the proposed controller for frequencies of 10 Hz and 15 Hz is bounded within ± 0.01 (μm) for both x- and y-axes which similar with low frequency (5 Hz) as shown in Figs. 15 and 18.

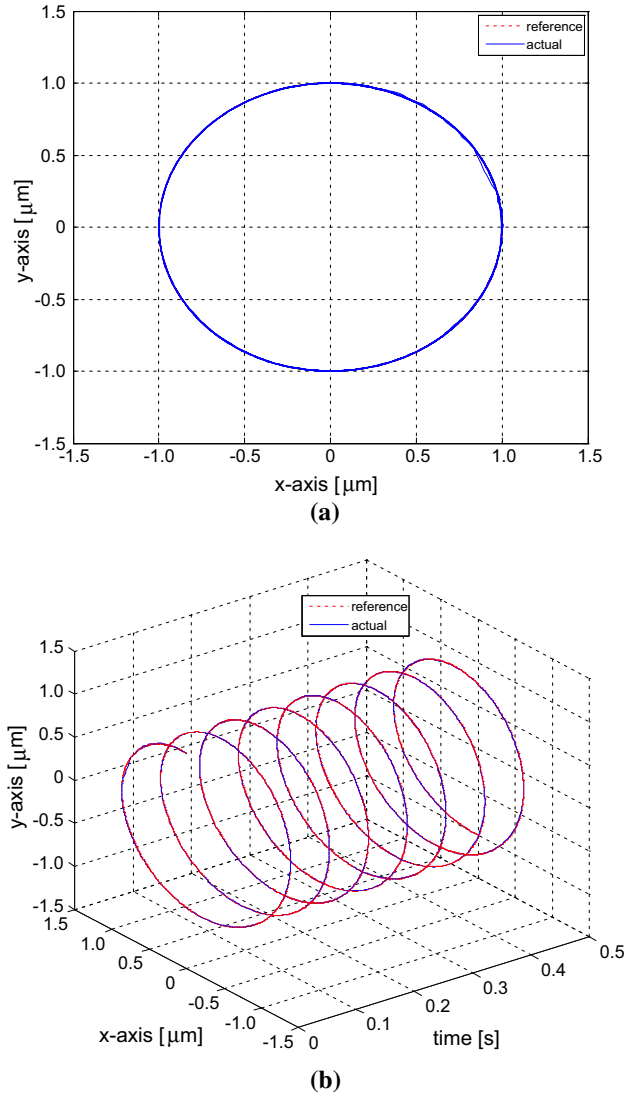

Fig. 19 Circular trajectory tracking response with frequency of 15 Hz using EBSMC in **a** 2D and **b** 3D

The ability of the proposed EBSMC system for the micromanipulation to track accurately the desired circle trajectory can be observed in the spatial curved shown in Figs. 16 and 19.

5 Conclusion

In this paper, a robust chattering free backstepping sliding mode controller is successfully developed for trajectory tracking of a 2-DOF piezo-actuated micromanipulation system. First, the mathematical model of the 2-DOF piezo-actuated micromanipulation system is introduced. Then, the proposed robust control system comprises a backstepping and a switching function is developed. The backstepping control design is derived based on Lyapunov function, so that the stability of the system can be guaranteed, while switching function is used to attenuate the effects caused by uncertainties. In order to eliminate the chattering phenomena, the sign function is replaced by a simple fuzzy system. Finally, the developed control scheme is applied to the 2-DOF piezo-actuated micromanipulation system. Simulation results show that a satisfactory control performance can be achieved by using the developed control system. Furthermore, it can be seen that a fuzzy system can be utilized to eliminate a chattering phenomena in the control inputs of the BSMC. In the future, the method provided can be utilized to deal with control problems of the piezo-actuated micromanipulation system with chaotic behavior.

Acknowledgements This work is supported by the Universiti Teknologi Malaysia Post-Doctoral Fellowship Scheme for the project 'A Control Design of a Piezoelectric Actuator for Bio-manipulation Systems.'

References

Acar C, Murakami T (2008). Underactuated two-wheeled mobile manipulator control using nonlinear backstepping method. In: proceedings of 34th annual conference of the IEEE industrial electronics society. pp 1680–1685

Adriaens HJMTA, de Koning WL, Banning R (1999). Feedback-linearization control of a piezo-actuated positioning mechanism. In: proceedings of european control conference (ECC). pp 1982–1987

Ahmad I, Abdurraqeeb AM (2017) H∝ control design with feed-forward compensator for hysteresis compensation in piezoelectric actuators. Automatika 57(3):691–702

Astrom KJ, Wittenmark B (1995) Adaptive Control. Addison-Wesley, New York

Badr BM, Ali WG (2010) Nano positioning fuzzy control for piezoelectric actuators. Int J Eng Technol 10:70–74

Bai R, Tong S, Karimi HR (2013) Modeling and backstepping control of the electronic throttle system. Math Probl Eng 87:1–6

Čas J, Škorc G, Šafarič R (2010) Neural network position control of XY piezo actuator stage by visual feedback. Neural Comput Appl 19(7):1043–1055

Chan CY, Nguang SK (2002) Backstepping control for a class of power systems. Syst Anal Model Simul 42(6):825–849

de Oliveira AS, da Costa Ferreira D, Chavarette FR, Peruzzi NJ, Marques VC (2015) Piezoelectric optimum placement via LQR controller. Adv Mater Res 1077:166–171

Ding B, Li Y, Xiao X, Tang Y (2016) Optimized PID tracking control for piezoelectric actuators based on the Bouc–Wen model. In: proceedings of IEEE international conference on robotics and biomimetics (ROBIO). pp 1576–1581

Elahinia M, Chen Y, Qiu J, Palacios J, Smith EC (2012) Tracking control of piezoelectric stack actuator using modified Prandtl-Ishlinskii model. J Intell Mater Syst Struct 24(6):753–760

Huang YC, Lin DY (2004) Ultra-fine tracking control on piezoelectric actuated motion stage using piezoelectric hysteretic model. Asian J Control 6(2):208–216

Ikhouane F, Rodellar J (2005) On the hysteretic Bouc–Wen model. Nonlinear Dyn 42(1):79–95

Krstic M, Kanellakopoulos I, Kokotovic P (1995) Nonlinear and adaptive control design, vol 222. Wiley, New York

Lee S-H, Royston TJ, Friedman G (2000) Modeling and compensation of hysteresis in piezoceramic transducers for vibration control. J Intell Mater Syst Struct 11(10):781–790

Lee G, You K, Kang T, Yoon KJ, Lee JO, Park JK (2010) Modeling and design of H-Infinity controller for piezoelectric actuator LIPCA. J Bionic Eng 7(2):168–174

Li Y, Xu Q (2010) Adaptive sliding mode control with perturbation estimation and PID sliding surface for motion tracking of a piezo-driven micromanipulator. IEEE Trans Control Syst Technol 18(4):798–810

Li P, Yan F, Ge C, Zhang M (2012) Ultra-precise tracking control of piezoelectric actuators via a fuzzy hysteresis model. Rev Sci Instrum 83(8):085114

Liang Y, Liu Y (2012) Backstepping control for nonlinear systems of offshore platforms. J Theor Appl Inf Technol 45(2):468–471

Lin C-J, Yang S-R (2006) Precise positioning of piezo-actuated stages using hysteresis-observer based control. Mechatronics 16(7):417–426

Lin J, Chiang H, Lin C (2011) Tuning PID control parameters for micro-piezo-stage by using grey relational analysis. Expert Syst Appl 38(11):13924–13932

Liu V-T (2012) Self-tuning Neuro-PID controller for piezoelectric actuator. Adv Sci Lett 14(1):141–145

Liu Y, Shan J, Gabbert U, Qi N (2013) Hysteresis and creep modeling and compensation for a piezoelectric actuator using a fractional-order Maxwell resistive capacitor approach. Smart Mater Struct 22(11):115020

Low T, Guo W (1995) Modeling of a three-layer piezoelectric bimorph beam with hysteresis. J Microelectromech Syst 4(4):230–237

Onawola OO, Sinha S (2011) A feedback linearization approach for panel flutter suppression with piezoelectric actuation. J Comput Nonlinear Dyn 6(3):031006

Payam AF, Fathipour M, Yazdanpanah MJ (2009). A backstepping controller for piezoelectric actuators with hysteresis in nanopositioning. In: proceedings of 4th IEEE international conference on nano/micro engineered and molecular systems (NEMS). pp 711–716

Rakotondrabe M (2011) Bouc–Wen modeling and inverse multiplicative structure to compensate hysteresis nonlinearity in piezoelectric actuators. IEEE Trans Autom Sci Eng 8(2):428–431

Ranaweera KMIU, Senevirathne KAC, Weldeab MK, Karimi HR (2013) Backstepping control design for a semiactive vehicle suspension system equipped with magnetorheological rotary brake. Int J Control Theory Appl 6(1):15–27

Shabaninia F, Mavaddat M (2014) Identification and control for a single-axis PZT nanopositioner stage. Univ J Mech Eng 2(4):132–137

Shen JC, Jywe WY, Liu CH, Jian YT, Yang J (2008) Sliding-mode control of a three-degrees-of-freedom nanopositioner. Asian J Control 10(3):267–276

Stakvik JÅ, Ragazzon MR, Eielsen AA, Gravdahl JT (2015) On implementation of the Preisach model: identification and inversion for hysteresis compensation. Model Identif Control 36(3):133–142

Svečko R, Kusić D (2015) Feedforward neural network position control of a piezoelectric actuator based on a BAT search algorithm. Expert Syst Appl 42(13):5416–5423

Thomas ME, Gopinath A (2016) LQR Control of Piezoelectric Actuators. Int Res J Eng Technol 3(7):96–102

Toader A, Ursu I (2007) Backstepping control synthesis for hydrostatic type flight controls electrohydraulic actuators. Ann Univ Craiova Ser Autom Comput Electron Mechatron 4(31):1

Wai R-J (2007) Fuzzy sliding-mode control using adaptive tuning technique. IEEE Trans Ind Electron 54(1):586–594

Witkowska A, Śmierzchalski R (2007) The use of backstepping method to ship course controller. TransNav Int J Mar Navig Saf Sea Transp 1(3):313–317

Xiao S, Li Y (2014) Dynamic compensation and H∞ control for piezoelectric actuators based on the inverse Bouc–Wen model. Robot Comput Integr Manuf 30(1):47–54

Xie WF, Fu J, Yao H, Su CY (2009) Neural network-based adaptive control of piezoelectric actuators with unknown hysteresis. Int J Adapt Control Signal Process 23(1):30–54

Xu Q (2014) Digital sliding-mode control of piezoelectric micropositioning system based on input–output model. IEEE Trans Ind Electron 61(10):5517–5526

Yang L, Li Z, Sun G (2014) Nano-positioning with sliding mode based control for piezoelectric actuators. In: Proceedings of International Conference on Mechatronics and Control (ICMC). pp 802–807

Youssef AMM (2013) Optimized PID tracking controller for piezoelectric hysteretic actuator model. World J Model Simul 9(3):223–234

Yu Y, Naganathan N, Dukkipati R (2002) Preisach modeling of hysteresis for piezoceramic actuator system. Mech Mach Theory 37(1):49–59

Zhou M, Wang J (2013) Research on hysteresis of piezoceramic actuator based on the Duhem model. Sci World J 2013:1–6